

# NO<sub>x</sub> emissions prediction for natural gas engines with fuel quality variations

G. Peureux<sup>\*,1</sup>, S. Carpentier<sup>1</sup>, G. Lartigue<sup>1</sup>

<sup>1</sup>CRIGEN, GDF SUEZ, 361 avenue du Président Wilson, 93 210 La Plaine Saint-Denis, France

## Abstract

The purpose of this study focuses on the prediction of NO emissions out of a spark ignition engine fueled with various compositions of natural gas. Based on the Zeldovich mechanism, a dedicated post-processor code was coupled with an existing simulation tool that was developed to predict engine output power and emissions when fueled with various compositions of natural gas. Three methods were tested for the initialization of NO concentration in the currently burning zone for each time step during the engine cycle. Results led to the choice of a specific level of mixing within the burnt gases that presents realistic trends in emissions with engine parameters and fuel composition variations.

## Introduction

In nowadays' energy context with high oil prices, Compressed Natural Gas (CNG) appears to be a cheap alternative fuel, more sustainable (longer-term fossil resources than oil) and compatible with the biomethane use (produced from a wide range of bio-wastes and raw biomass). Vehicles fuelled and powered by CNG have less impact on the environment (23% reduction in CO<sub>2</sub> emissions in comparison to gasoline and lower local pollutants emissions). Finally, natural gas supply and markets suffer less than the oil supply and markets as natural gas resources are well spread over the world and located in safe and stable areas.

As natural gas is distributed to end-customers through an international interconnected network, with various injection ports all along the gas grid and different origins of supply, its composition may vary all along the grid and over the time. The need for a security of supply requires various sources of natural gas which could lead to an increasing risk of variation of its composition / quality at the delivery point.

Fluctuations in fuel composition may particularly affect the combustion quality at lean operating limit conditions. Thus, the stability of fuel specifications is an important parameter for engine manufacturers to achieve the best compromise between high level of power, low consumption, low emissions and the knock prevention.

Cars and trucks manufacturers are not experts in natural gas, and bringing them further skills is a condition to the success of the NGV market development. In order to help to optimize their CNG engines, GDF SUEZ has developed a simulation tool based on its experience of natural gas combustion to predict the impact of natural gas composition on power output and exhaust emissions. Its purpose is to analyze the influence of gas quality on the engine behavior, and how throttling, spark timing, air / fuel ratio or recirculation of burnt gases can help, keeping a constant power output (with a constant driving feeling, comparable to a commercial gasoline vehicle) and satisfactory exhaust emissions (with respect to current

and future pollution standards) over a wide range of natural gas compositions.

This tool is a time-scaled 0 dimensional calculation code which was first written in Fortran 90 [1]. The combustion part consists in a two-zone thermodynamic model. Flow description and thermodynamics are calculated thanks to usual models for 0 dimensional codes [2], with a high focus on the impact of quality variations of natural gas as a multi component gaseous fuel.

Today, this former Fortran 90 homemade model has been implemented in an industrial platform well spread over the car industry: LMS Imagine.Lab AMESim®. The objective is then to use this tool in collaborative research programs to strengthen interactions with car manufacturers and to take a better hold on the NGV market development.

Nevertheless, this paper focuses on the former Fortran 90 code that was developed by GDF SUEZ. The ability of the new platform to predict NO<sub>x</sub> emissions will be discussed in later works.

## Specific Objectives

The present study focuses on the development of a NO post-processor coupled with the natural gas engine simulation tool [1]. Three models were implemented in this post-processor. The simulation results were compared to experimental data available for a light duty engine fueled with various compositions of natural gas.

## Experimental facilities

Engine tests were conducted on a light duty spark ignition base model engine designed for both gasoline and natural gas operations. This engine has a capacity of 1.4 liter with a volumetric compression ratio of 10:1.

The test rig main characteristics are: maximum torque of 1400 Nm, maximum rotational speed of 8000 rpm, maximum power of 255 kW (345 hp).

Natural gas composition is adjusted with an in-line gas mixer. Flow is measured with a Coriolis mass flow meter. Dedicated mass flow meters control adjunctions of pure nitrogen, ethane, propane and butane to base

---

\* Corresponding author: [guillaume.peureux@gdfsuez.com](mailto:guillaume.peureux@gdfsuez.com)  
Proceedings of the European Combustion Meeting 2009

pure methane fuel. This system, presented by figure 1, enables to create a wide range of natural gas compositions with a restricted number of gas bottles.

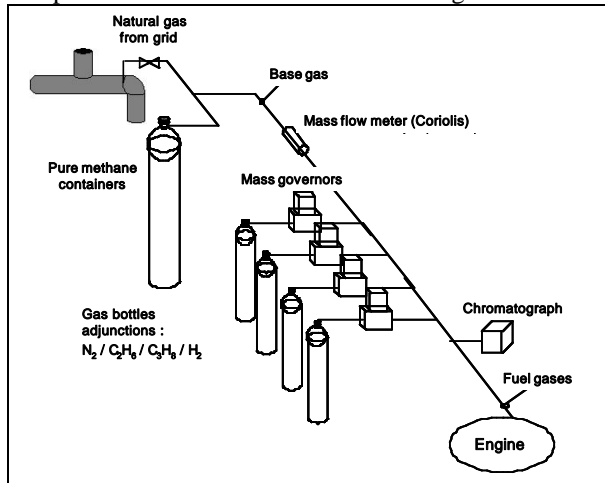


Fig. 1: Test rig in-line mixer overview

This test bench enables accurate mixing of five pure gas mixtures (including methane) and also the injection of a liquid fuel (such as butane) in the blend.

Combustion products  $\text{NO}_x$ ,  $\text{C}_n\text{H}_m$ ,  $\text{O}_2$ ,  $\text{CO}$ ,  $\text{CO}_2$ ,  $\text{CH}_4$  are measured. An online chromatograph is used to check fuelled natural gas composition before every test. Instantaneous cylinder pressure, inlet and outlet gases temperatures, inlet and outlet cooling water temperatures, static pressure in the intake manifold and various other parameters are measured.

Engine tests included more than a thousand different points with variations in natural gas composition, load, fuel-air equivalence ratio, spark timing and engine speed.

An average natural gas composition was first chosen, and the other natural gas compositions were obtained with addition, either separately or jointly, of ethane, propane, butane, nitrogen and hydrogen. Hydrogen was used for tests with Hythane® composition: 20% of hydrogen in volume with 80% of natural gas.

### Combustion model calibration procedure

Before testing the various NO models that are described further in this study, calibration of the simulation tool had to be achieved with care so the program would correctly calculate the combustion phase of the engine cycle. Thus, calibration of the combustion parameters in the engine combustion code was achieved with care.

Regarding the combustion model itself, previous works were dedicated to laminar flame speed calculations for natural gas mixtures over temperature and pressure ranges where experimental data are not easily available. A calibration of a turbulent constant in the combustion model and the delay between spark ignition and start of combustion led to good estimations of in-cylinder pressure evolution which is the first in-cylinder parameter influenced by variations in the combustion process. The chosen parameters for

calibration were: cycle maximum pressure level, crank timing over the cycle and indicated mean effective pressure.

Figure 2 shows a comparison between cylinder curves from test and simulation results. It details the significance of calibration parameters over the various phases of engine cycle.

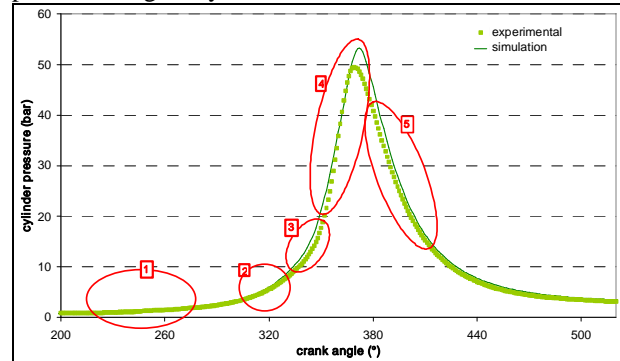


Fig. 2: Cylinder pressure: comparison between experimental data and simulation result - simulation key parameters to reproduce experimental behavior

The steps for the combustion model calibration that are highlighted in figure 2 are:

1. in cylinder mass: mass calibration is achieved through residual gases rate estimation. In this study, after a calibration for each tested point, a correlation was determined and used for all following model calibration steps. It does not take into account some particularities of each point such as exhaust temperature, or acoustic waves' magnitude.

2 and 5. start of compression phase and expansion phase: at this step, thermal losses have to be calibrated. Error in pressure estimation can be induced here by in cylinder mass estimation error, and then, also by:

- compression ratio uncertainty due to manufacturer's production tolerance.
- thermal losses, because the calibration is averaged over all experimental data from the tests,
- ideal gases hypothesis may not be representative of real behavior.

3. start of combustion: the delay between spark ignition and the start of combustion has to be calibrated.

4. turbulent flow: a calibration is done for at the same time as for start of combustion phase, for the turbulent parameter so as to get best compromise. Non-physical solutions are excluded by the convergence criterion, and by post calculation control of calibrated data.

5. expansion phase: thermal losses are also calibrated at expansion phase (see 2.). During this phase, all cumulated errors are gathered. Same reasons as for compression phase may explain specific errors (not induced by previous calibrations) in this phase.

For the study of NO emissions out of the engine, closed valve calculations were performed. The main parameter that was fitted in this study is the turbulent flow constant of the model.

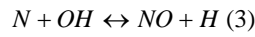
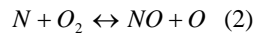
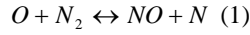
With lack of data over the instantaneous pressure in the intake manifold, a residual burnt gases rate was calibrated over 20% of all experimental data in order to get better accuracy over in-cylinder mixture mass during closed valve phases in the engine cycle. Dependency over load and engine speed was then taken into account to create a formula describing the evolution of this residual burnt gases rate over experimental data. In-cylinder mass was determined with this formula.

With lack of data over wall temperature of the engine, thermal losses were put to default values without introducing dependency over load. Thus, evaluation of the NO models was focused on error distribution over the simulated points, and not over error itself.

### NO emissions modeling

The NO model implemented in the post-processor is based on the well-known Zeldovich mechanism, with constants available from the literature: [3,4].

This NO mechanism consists of the following reactions, [5-12]:



These reactions' constants can be written in the following form:

$$K = A \cdot T^B \cdot e^{-\frac{E}{RT}}$$

Formation constants are usually quoted  $K^+$  (forward direction) and dissociation constants  $K^-$  (backward direction). A, B and E constant values are gathered in Table 1.

| (i) | $K^+$                |   |        | $K^-$                |     |        |
|-----|----------------------|---|--------|----------------------|-----|--------|
|     | A                    | B | E      | A                    | B   | E      |
| 1   | $1,36 \cdot 10^{14}$ | 0 | 315900 | $3,27 \cdot 10^{12}$ | 0,3 | 0      |
| 2   | $6,4 \cdot 10^9$     | 1 | 26300  | $1,5 \cdot 10^9$     | 1   | 162100 |
| 3   | $6,8 \cdot 10^{13}$  | 0 | 0      | $2,0 \cdot 10^{14}$  | 0   | 196600 |

Table 1: Formation and dissociation constants for NO mechanism: [3,4], units: A ( $\text{cm}^3/\text{mol}\cdot\text{s}$ ), B (-), E ( $\text{J}/\text{mol}$ )

For each of these reactions,  $R_i$  is the reaction rate at equilibrium of reaction (i):

$$R_1 = K_1^+ \cdot [N_2]_e \cdot [O]_e = K_1^- \cdot [NO]_e \cdot [N]_e$$

$$R_2 = K_2^+ \cdot [O_2]_e \cdot [N]_e = K_2^- \cdot [NO]_e \cdot [O]_e$$

$$R_3 = K_3^+ \cdot [OH]_e \cdot [N]_e = K_3^- \cdot [NO]_e \cdot [H]_e$$

With:

- $K_i$  reaction kinetic constant of reaction (i) ( $\text{cm}^3/\text{mol}\cdot\text{s}$ ),
- $[X]_e$  concentration at equilibrium of species X ( $\text{mol}/\text{cm}^3$ ),
- $R_i$  reaction rate at equilibrium for reaction (i) ( $\text{mol}/\text{cm}^3\cdot\text{s}$ ).

Among the species involved in these reactions, Kesgin [5] states that part of them can be regarded close to equilibrium since they are reactant of other

combustion reactions which are much faster than (1), (2) and (3): O,  $O_2$ , OH and H. NO and N cannot be considered close to equilibrium. Choosing  $\alpha$  and  $\beta$  variables as follows,

$$\alpha = \frac{[NO]}{[NO]_e} \quad \text{and} \quad \beta = \frac{[N]}{[N]_e}$$

Following Kesgin [5], NO and N formation rates are written here as a function of time:

$$\frac{d[NO]}{dt} = R_1 + \beta(R_2 + R_3) - \alpha(\beta R_1 + R_3 + R_3)$$

$$\frac{d[N]}{dt} = R_1 + \alpha(R_2 + R_3) - \beta(\alpha R_1 + R_2 + R_3)$$

Considering quasi-steady state hypothesis for N, we can write NO formation rate as:

$$\frac{d[NO]}{dt} = \frac{2 \cdot R_1 \cdot (1 - \alpha^2)}{\left(\alpha \cdot \frac{R_1}{R_2 + R_3} + 1\right)}$$

Three different models were tested using this approach in this study. The difference between these models is the initialization value used for the solving of NO formation at each time step of the calculation: how front flame zone is mixing with previous burnt gases and how these burnt gases mix themselves:

- For model A, NO formation calculation in the new zone is initiated with the concentration of NO in the former zones that have been homogenized, as shown in figure 3,
- For model B, all burnt zones are mixed and have an homogenous repartition of NO previously created in the gases; this homogenized concentration of previous NO also initiates the burning zone calculation, as shown in figure 4,
- For model C, there is no transfer of matter between any zones; all zones have their own evolution, the currently burning zone is initiated with no NO, as shown in figure 5.

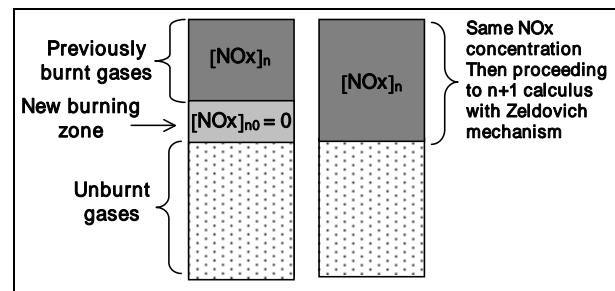


Fig. 3: Initialization of NO concentration for next calculation step in the burning zone and exhaust gases for model A – the currently burning zone starts with the same concentration of NOx as the current concentration in the previously burnt zones.

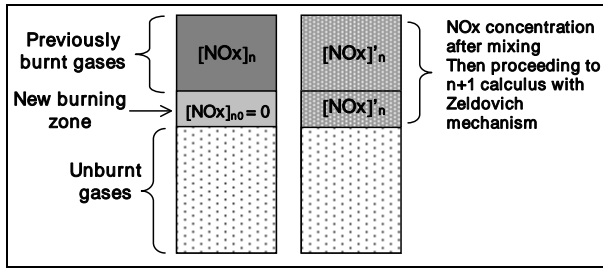


Fig. 4: Initialization of NO concentration for next calculation step in the burning zone and exhaust gases for model B – burnt gases mix with the currently burning zone.

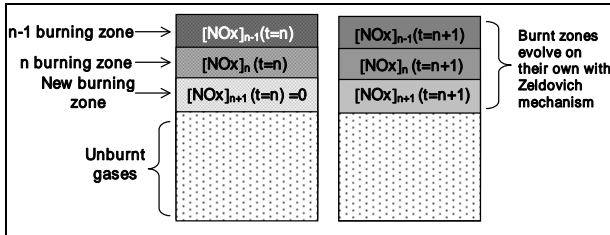


Fig. 5: Initialization of NO concentration for next calculation step in the burning zone and exhaust gases for model C – there is no mixing within the burnt gases.

The mass of burnt gases created during this time step is then stored and considered as a burnt gas zone. The temperature and pressure in this zone evolve under the same conditions as the rest of the burnt gases.

## Results and Discussion

Among  $\text{NO}_x$  emissions out of the engine, NO emissions account for a high proportion of these. The same modeling is to be done with  $\text{NO}_2$  to increase accuracy. Before testing these various  $\text{NO}_x$  models, calibration of combustion parameters in the engine combustion code was achieved with care.

For the calculations with the NO models to evaluate, only the experimental tests that were simulated with lowest errors by the combustion code were chosen so as to reduce to the maximum the errors introduced by the previous phase of calibration of the combustion model.

NO calculations were then obtained on more than 130 experimental points. Results showed all emissions were underestimated. Main reason would be an overestimation of thermal losses through too high default values for thermal exchange constant in the dedicated correlation from Hohenberg [13], and the need to introduce a dependency between wall temperature and load variations. Figure 6 shows the distribution of NO emissions' underestimations by A, B and C models, with values of first and ninth deciles and their mean values. Despite of the lack of accuracy due to high thermal losses, the ability to give satisfactory tendencies predictions by the various models can be compared through these results. Distributions of errors are as follows:

- model A: mean error is 19%, while 80% of errors are included between 6.6% and 27%,

- model B: mean error is 25%, while 80% of errors are included between 17.7% and 30.8%,
- model C: mean error is 27.3%, while 80% of errors are included between 20.7% and 32.9%.

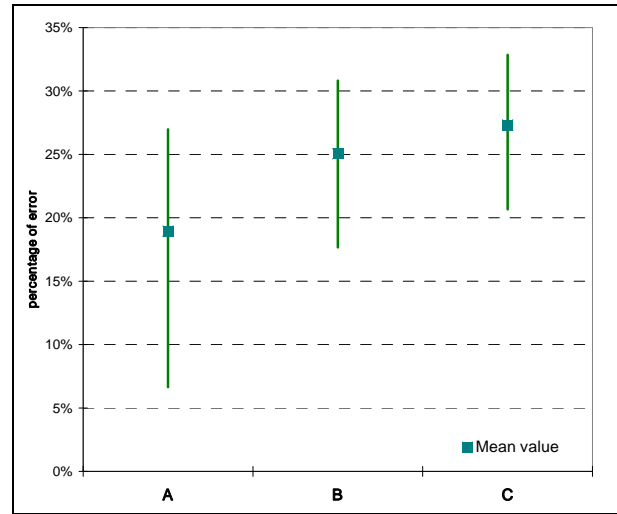


Fig. 6: Distribution of  $\text{NO}_x$  emissions underestimations by models A, B, and C: interval between first and ninth deciles, with mean values dots.

Model C gives best error distribution with the narrowest interval. Since B gives quite similar results, choice of the best NO prediction model between B and C models will be set with later works.

Figure 7 shows emissions predictions by model C over tests at full load with engine speed variations with two different natural gases compositions: Table 2.

|                           | NG1  | NG2  |
|---------------------------|------|------|
| $\text{CH}_4$             | 82.8 | 82.3 |
| $\text{C}_2\text{H}_6$    | 10.5 | 5.0  |
| $\text{C}_3\text{H}_8$    | 3.8  | 1.8  |
| $\text{C}_4\text{H}_{10}$ | 2.0  | 0.0  |
| $\text{N}_2$              | 0.9  | 10.9 |

Table 2: Example of 2 natural gas compositions tested

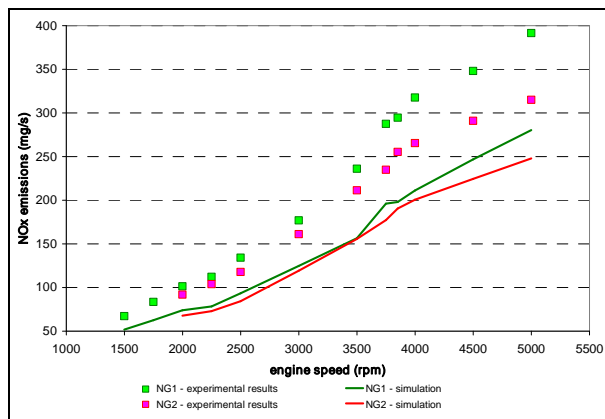


Fig. 7: NO<sub>x</sub> emissions at full load with engine speed variations: experimental data and simulations with model C for two natural gas compositions.

Tendencies in NO formation are well predicted over the simulated points, with respect to engine speed and gas quality variations.

### Conclusions

This study showed that the three models of NO emission based on the Zeldovich mechanism give satisfying levels of errors over the prediction. The third model in this work, with an initialization of NO concentration with a non-mixing of the burnt gases, gave most satisfying results with regard to the ability to predict tendencies while varying engine parameters and natural gas fuel composition.

As NO production is quite sensitive to temperature level in the burnt gas zone, predictions of NO emissions tendencies over all the simulated points give another confirmation on the relevance of the calculated temperature for burnt gases, and so the whole combustion model used over fuel quality variations.

Here remain works to be achieved over thermal losses through walls to be taken into account more accurately: dedicated calibration and introducing a dependency between wall temperature and load variations. Therefore, higher accuracy in the prediction of NO emissions out of the engine may be achieved through better prediction of thermal loss.

### Acknowledgements

The authors acknowledge the students N. Lurcel and O. Baudrand for their help with the preparation phase of this study. The authors also express their thanks to the colleagues of GDF SUEZ - CRIGEN for their helpful comments and advice during the manuscript preparation.

### References

- [1] C. Caillol, G. Berradi, G. Brecq, M. Ramspacher, P. Meunier, A simulation tool for evaluating gas composition effects on engine performance, 2004,
- [2] J. B. Heywood, Internal Combustion Engine Fundamentals, McGraw-Hill, New York, 1988,

- [3] C. Bowman. Kinetics of pollutant formation and destruction in combustion. Progress in Energy and Combustion Science, 1:33-45, 1975,
- [4] J. Miller, C. Bowman. Mechanism and modeling of nitrogen chemistry in combustion. Progress in Energy and Combustion Science, 15:287-338, 1989,
- [5] U. Kesgin, « Study on prediction of the effects of design and operating parameters on NO<sub>x</sub> emissions from a lean-burn natural gas engine », Energy Conversion and Management 44 (2003) 907-921, 2002,
- [6] U. Kesgin, « Genetic algorithm and artificial neural network for engine optimisation of efficiency and NO<sub>x</sub> emission », Fuel 83 (2004) 885-895, 2003,
- [7] C.D. Rakopoulos, E.G. Giakoumis, D.C. Kyritsis, Validation and sensitivity analysis of a two zone Diesel engine model for combustion and emissions prediction, Energy Conversion and Management 45 (2004) 1471-1495, 2003,
- [8] J.A. Caton, Detailed result for nitric oxide emission as determined from a multiple-zone cycle simulation for a spark-ignition engine, ASME-IDES 08-11, 2002,
- [9] J.A. Caton, Effects of burn rate parameters on nitric oxide emission for a park ignition engine: Results for a tree-zone, thermodynamic simulation, Department of Mechanical Engineering, Texas A&M University, 2003-01-0720, 2003,
- [10] R.S. Fletcher et J.B. Heywood, A model for nitric oxide emission from aircraft gas turbine engine, American Institute of Aeronautics and Astronautics, AIAA Paper n° 71-123, 1971,
- [11] W.P.J. Visser et S.C.A. Kluiters, Modelling the effects of operating conditions and alternative fuels on gas turbine performance and emissions, National Aerospace Laboratory NLR, NLR-TP-98629, 1998,
- [12] C. Caillol, Influence de la composition du gaz naturel carburant sur la combustion turbulente en limite pauvre dans les moteurs à allumage commandé, PhD thesis, Université de Provence, 2004,
- [13] G.F. Hohenberg, Advanced approaches for heat transfer calculations, SAE Paper, (790825), 1979.